

The variation in time t and space s of particle displacement in a wave is of the form

$$A \cos 2\pi \left(\frac{t}{T} - \frac{s}{\lambda} \right)$$

amplitude \nearrow

~~amplitude~~

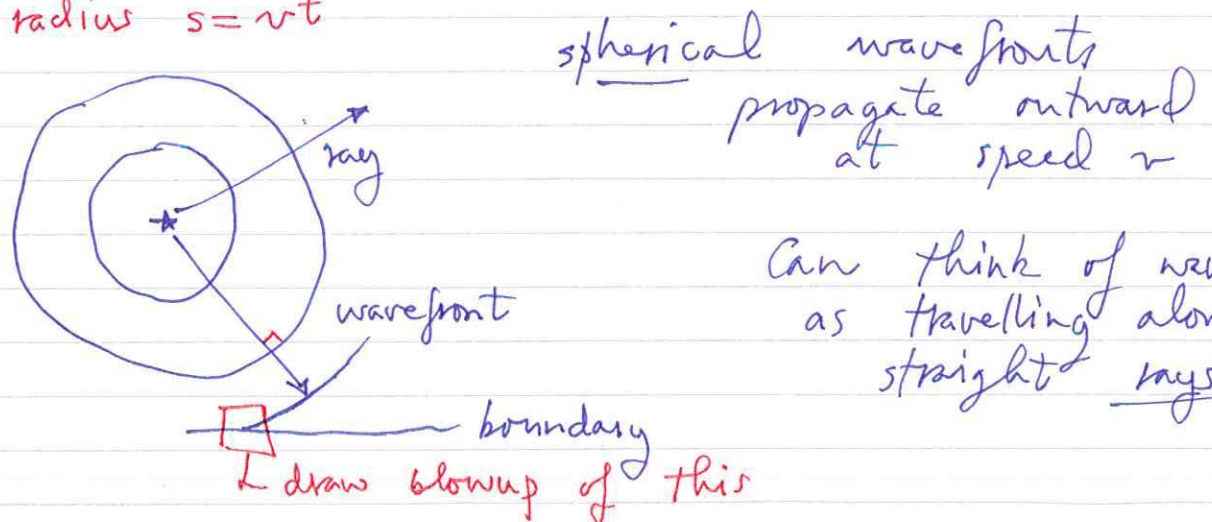
$T = \text{period}$
 $\lambda = \text{wavelength}$
 $s = \text{distance measured along ray}$
 $t = \text{time}$

Speed v (either α or β) = $\frac{\lambda}{T}$

$\lambda \leftarrow \text{wavelength}$
 $T \leftarrow \text{period}$

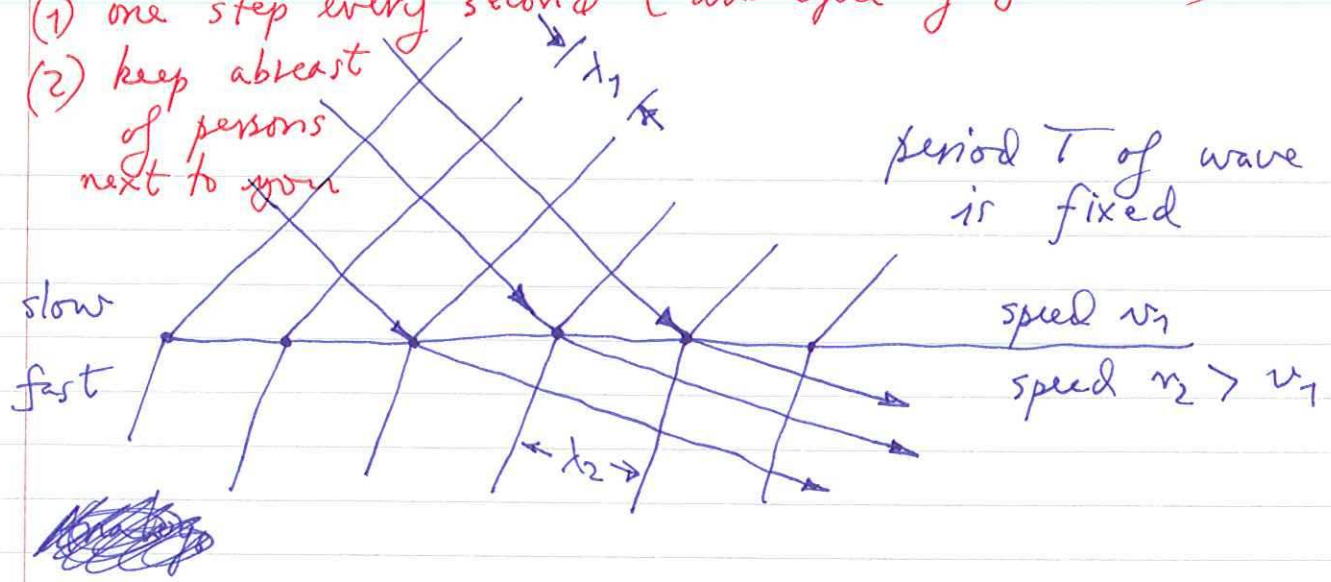
Consider the waves excited by an earthquake (regarded for the moment as a point source)

Thought experiment — homogeneous medium
 radius $s = vt$



What happens when a wave encounters a boundary between two materials?

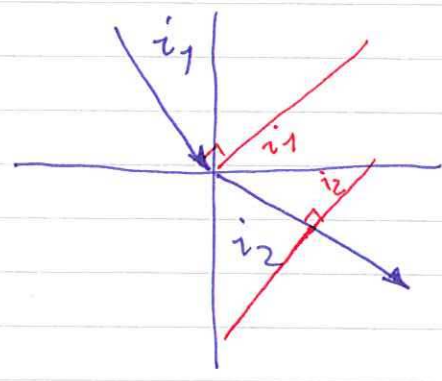
Drill sergeant gives 2 orders:
 (1) one step every second (analogue of fixed T)
 (2) keep abreast of persons next to you



Wave is refracted upward upon entering a faster medium

Analogy — think of lines of troops leaving a swamp and entering a blocktop parking lot

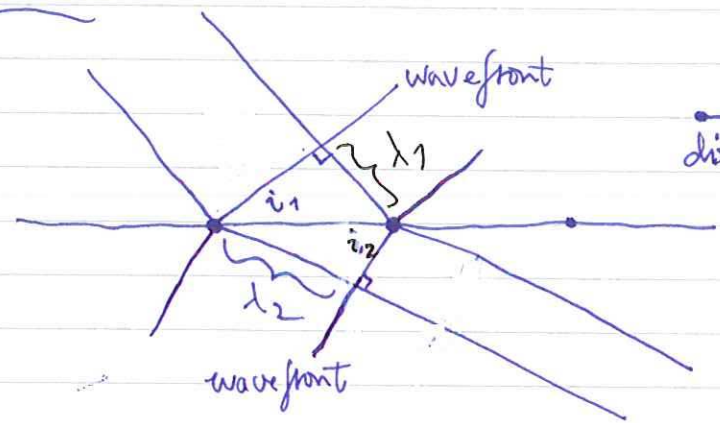
one step per second — small steps in swamp & big in parking lot



$$\frac{\sin i_1}{v_1} = \frac{\sin i_2}{v_2}$$

Snell's law of refraction

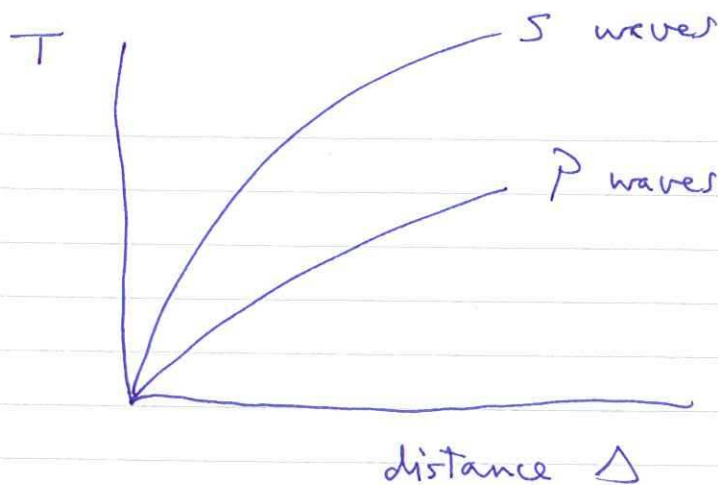
Derivation:



$$\text{distance} = \frac{\lambda_1}{\sin i_1} = \frac{\lambda_2}{\sin i_2}$$

$$\frac{\sin i_1}{v_1 T} = \frac{\sin i_2}{v_2 T}$$

↑ same ↑



In any little layer $dT = \frac{ds}{v}$ ← distance traveled

Total time : $T = \int \frac{ds}{v}$

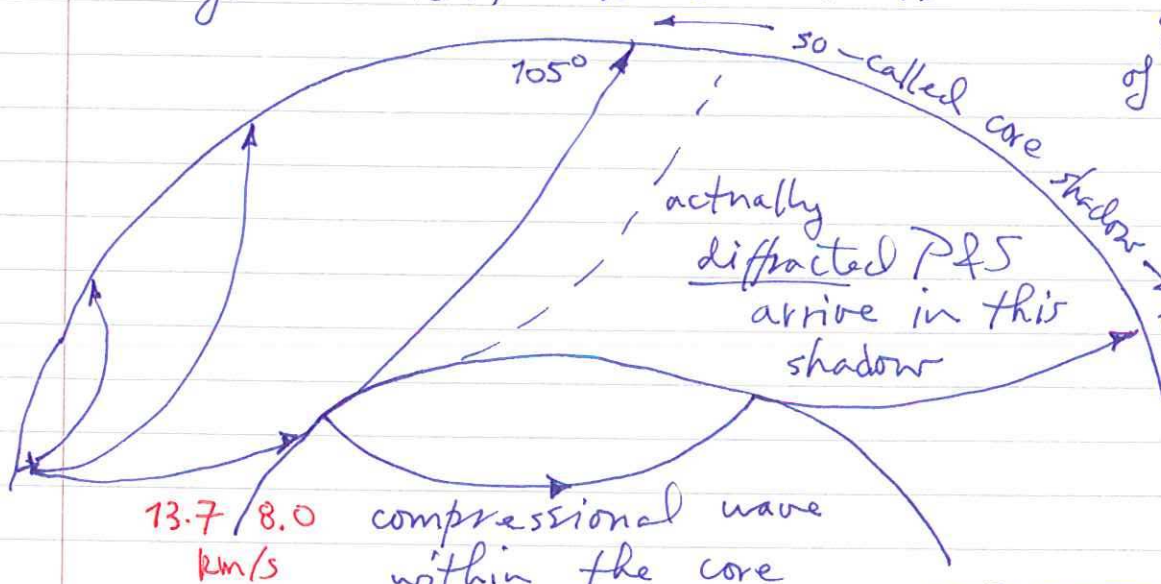
$T = \sum dT = \sum \frac{ds}{v}$
 $= \int \frac{ds}{v}$

the integral adds up all the dT's.

make each \sum look more like \int at 2900 km depth

Below the CMB S waves can no longer propagate. Furthermore P waves are refracted deep down into the core because of the decrease in v from 13.7 to 8.0 km/s

“that's all these is to integration”



give example of an ordinary shadow - has a diffuse edge due to diffraction

~~2900 km depth~~

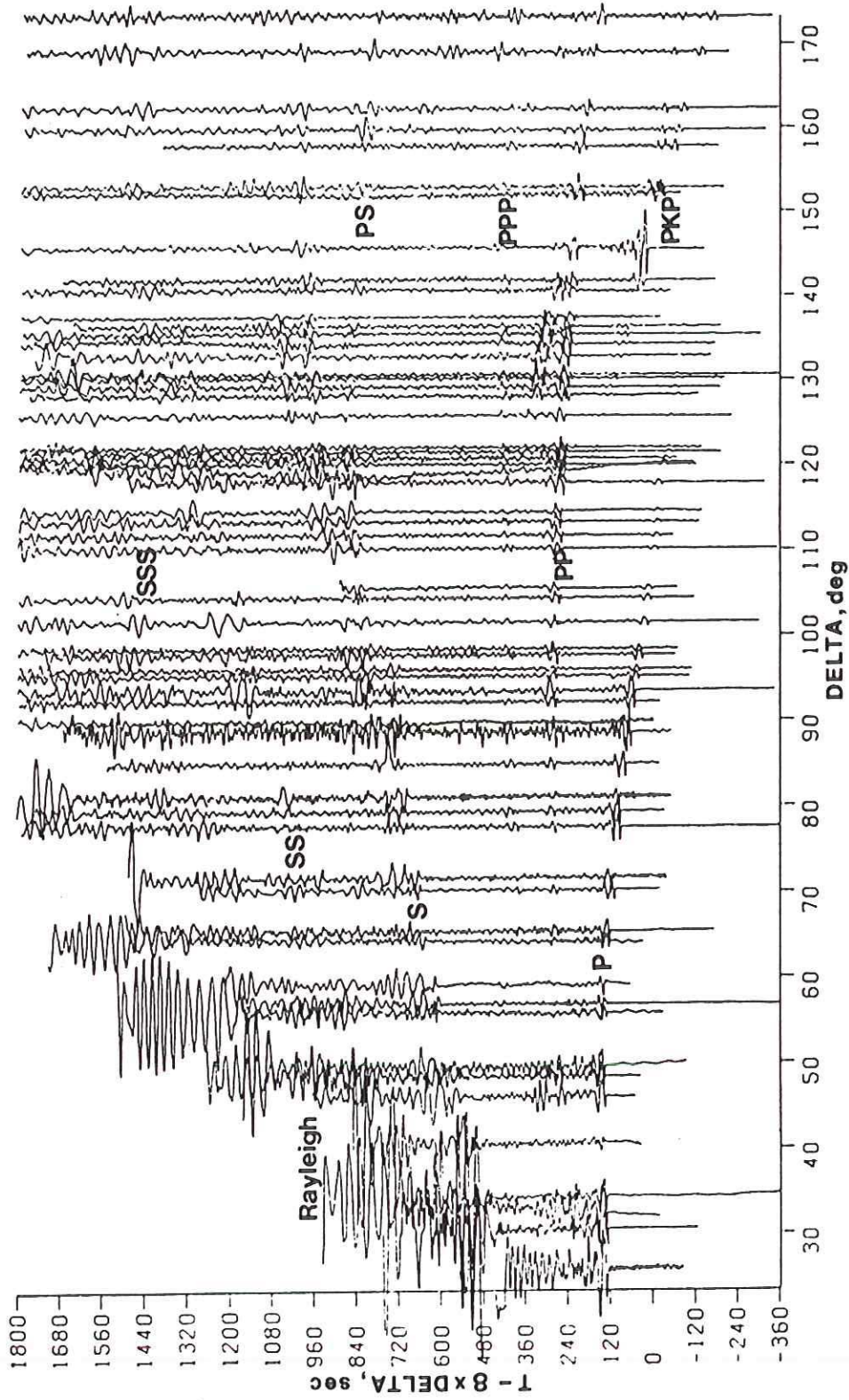
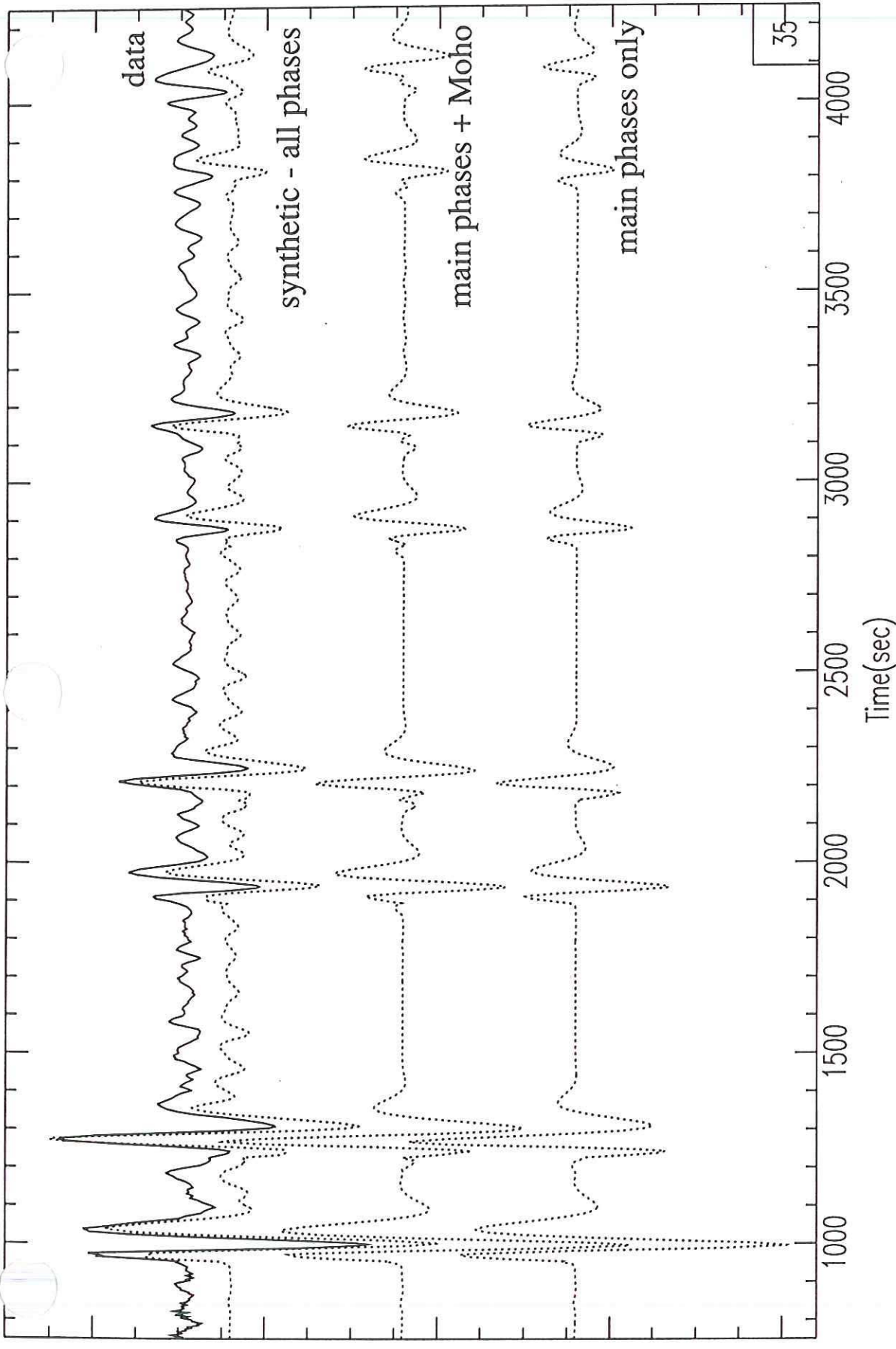


FIGURE 1.18 A collection of vertical-component seismograms for a single event that occurred near Sumatra, plotted at the angular distance to each station. The records are from the World Wide Standardized and Canadian Seismic Networks. Upward motion on each trace is toward the left. Note that coherent arrivals can be tracked from trace to trace. These define the travel-time behavior for different paths through the Earth. The start time of each trace has been reduced by a value of 8Δ s, where Δ is the angular distance. Thus, traces on the right begin much later than traces on the left. (Modified from Müller and Kind, 1976. Reprinted with permission of the Royal Astronomical Society.)



Example of radial component seismogram (low-passed at 100s) from the most western station in Bolivia (STO1), and comparison with synthetics. Traces are (from bottom): - CORE synthetic with main phases only. CORE synthetic with Moho phases included (note that Moho precursors alter the shape of sScS pulses, thus constraining the Moho depth). CORE synthetic with all discontinuities included. Additional phases seen are boundary interaction phases from D400, D600 and D230. Note that most of these phases are also seen in the data (top trace), allowing us to obtain single station path-averaged estimates of discontinuity depths.

246 SEISMIC WAVES AND THE STRUCTURE OF THE EARTH

how do we know these are there?

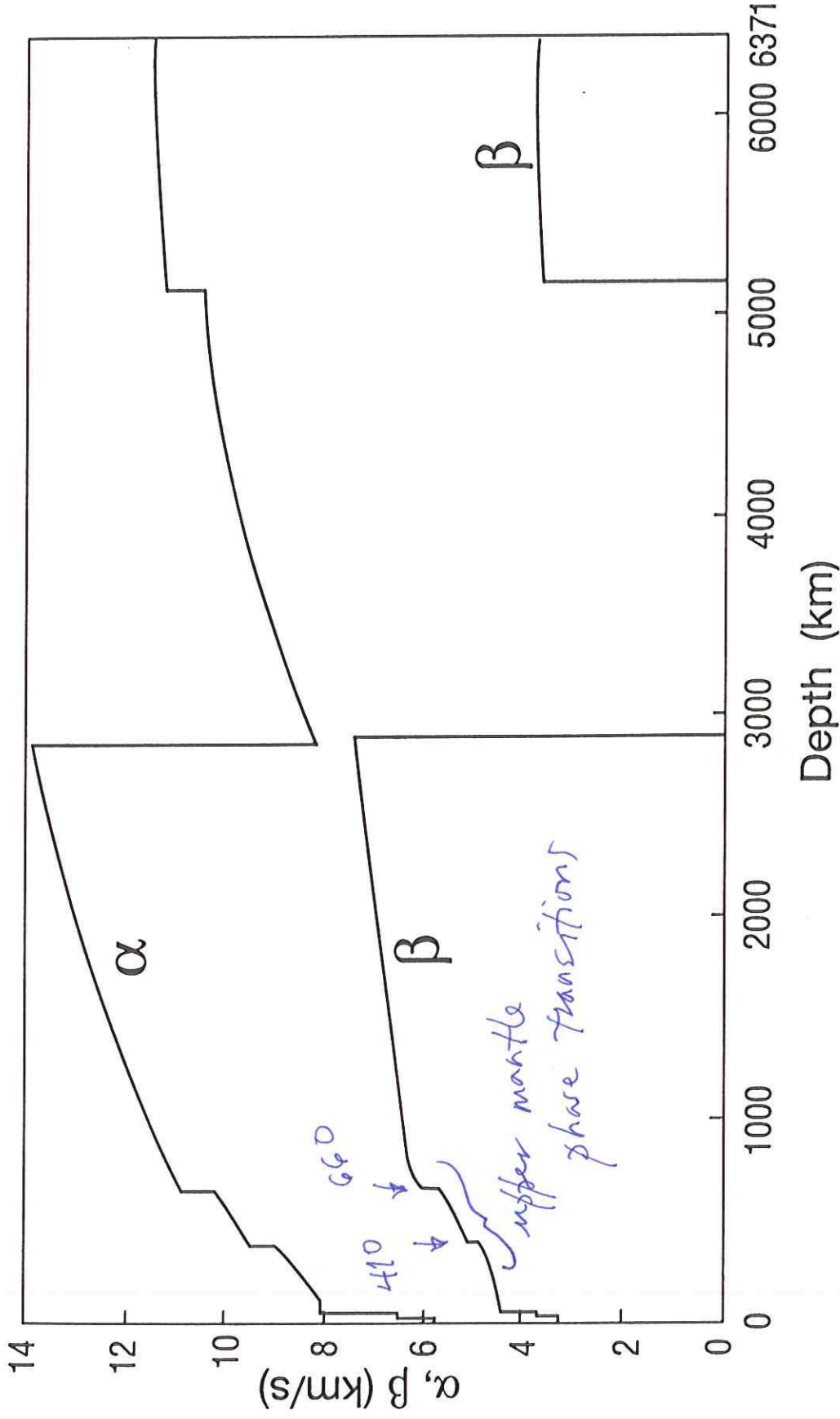


Figure 5.17 P and S wave speeds, α and β , in the iasp91 model of the Earth developed from body wave travel times (Kennett and Engdahl, 1991). Like several other recent Earth models, iasp91 is parameterized, in the sense of having wave speeds that are simple polynomial functions of radius over 11 independently fitted depth ranges.

A shear-velocity model of the mantle

circum-Pacific
donut of low velocity
 $\frac{\delta\beta}{\beta} \approx 3\%$ low

1389

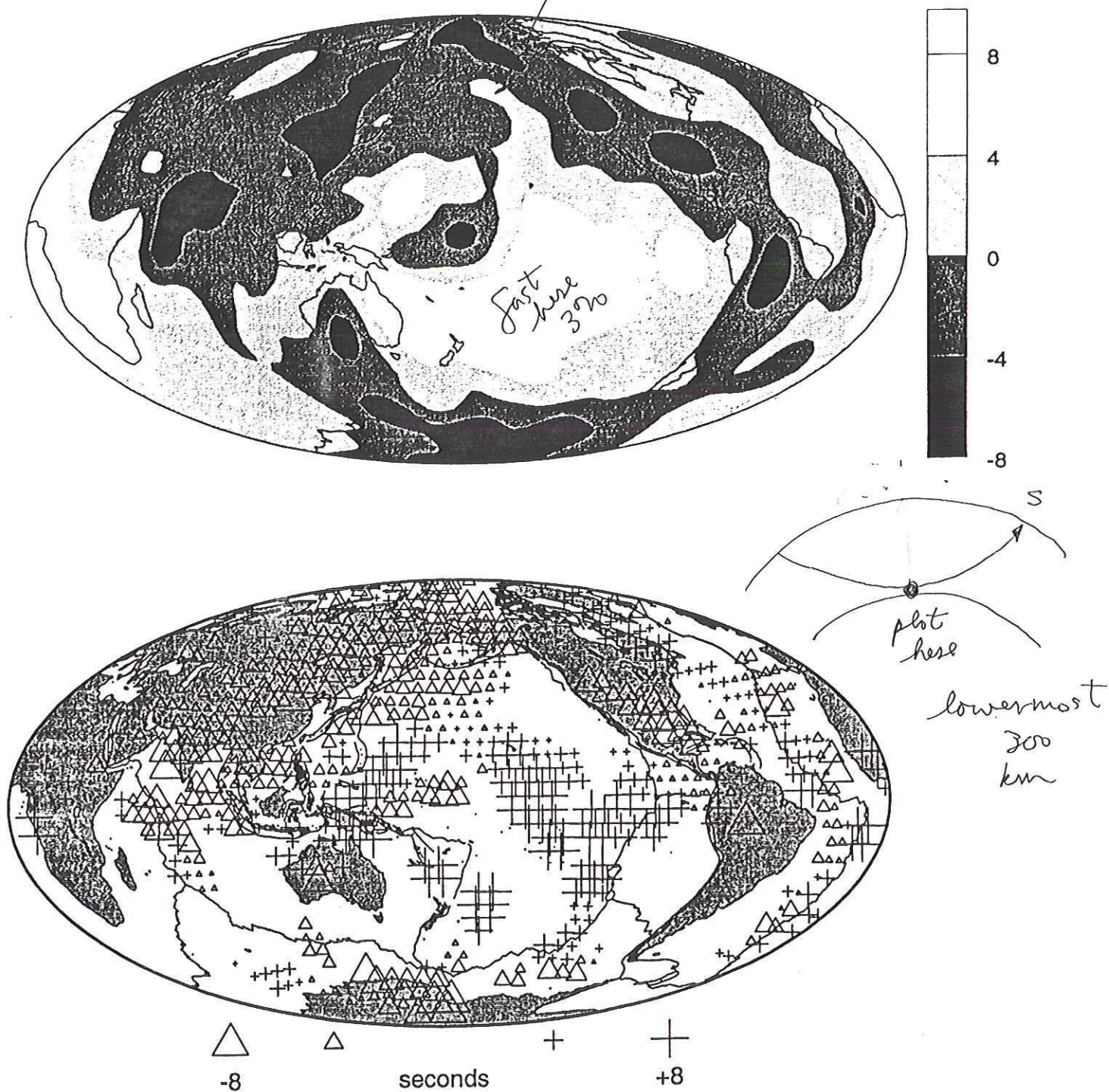
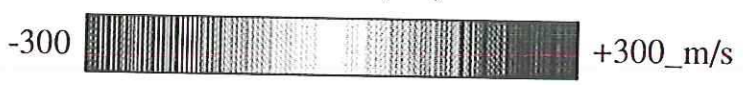
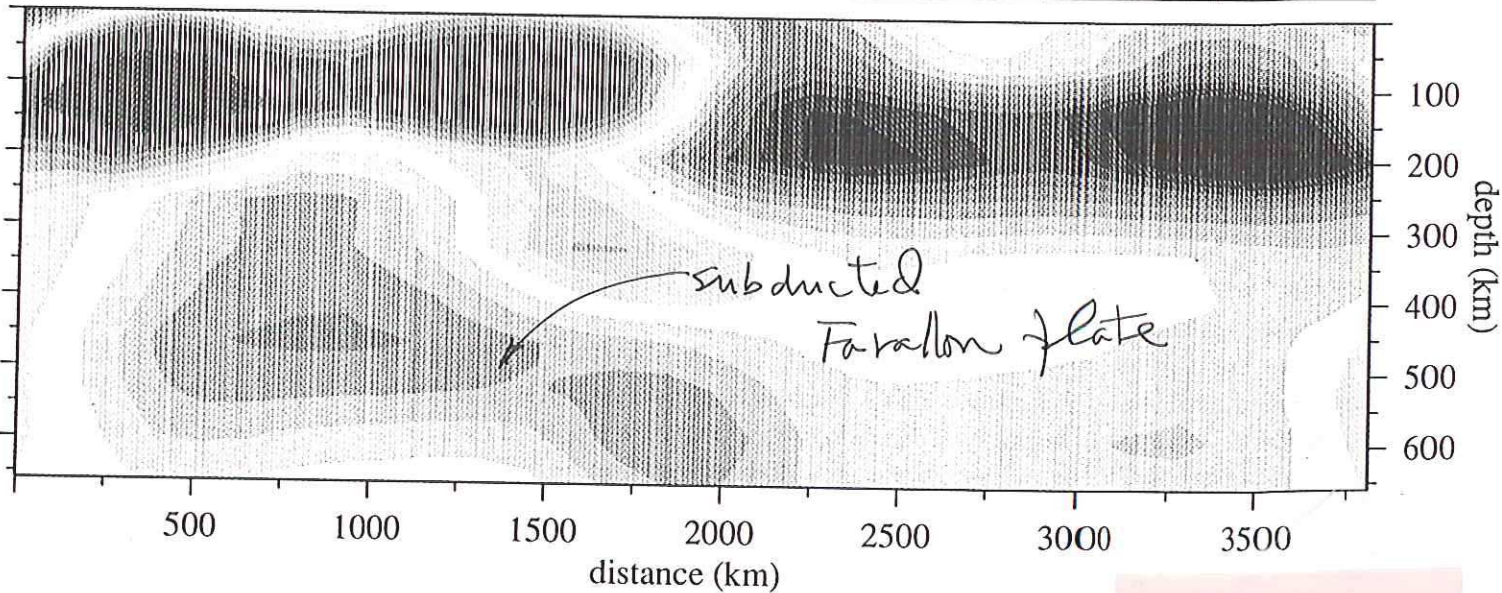
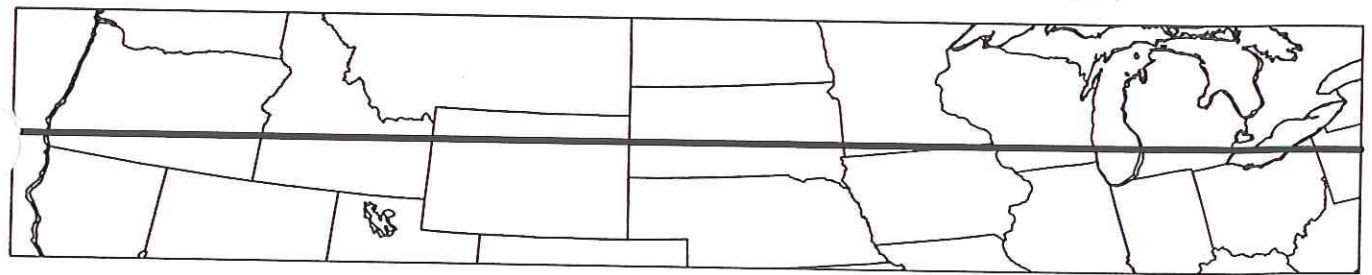
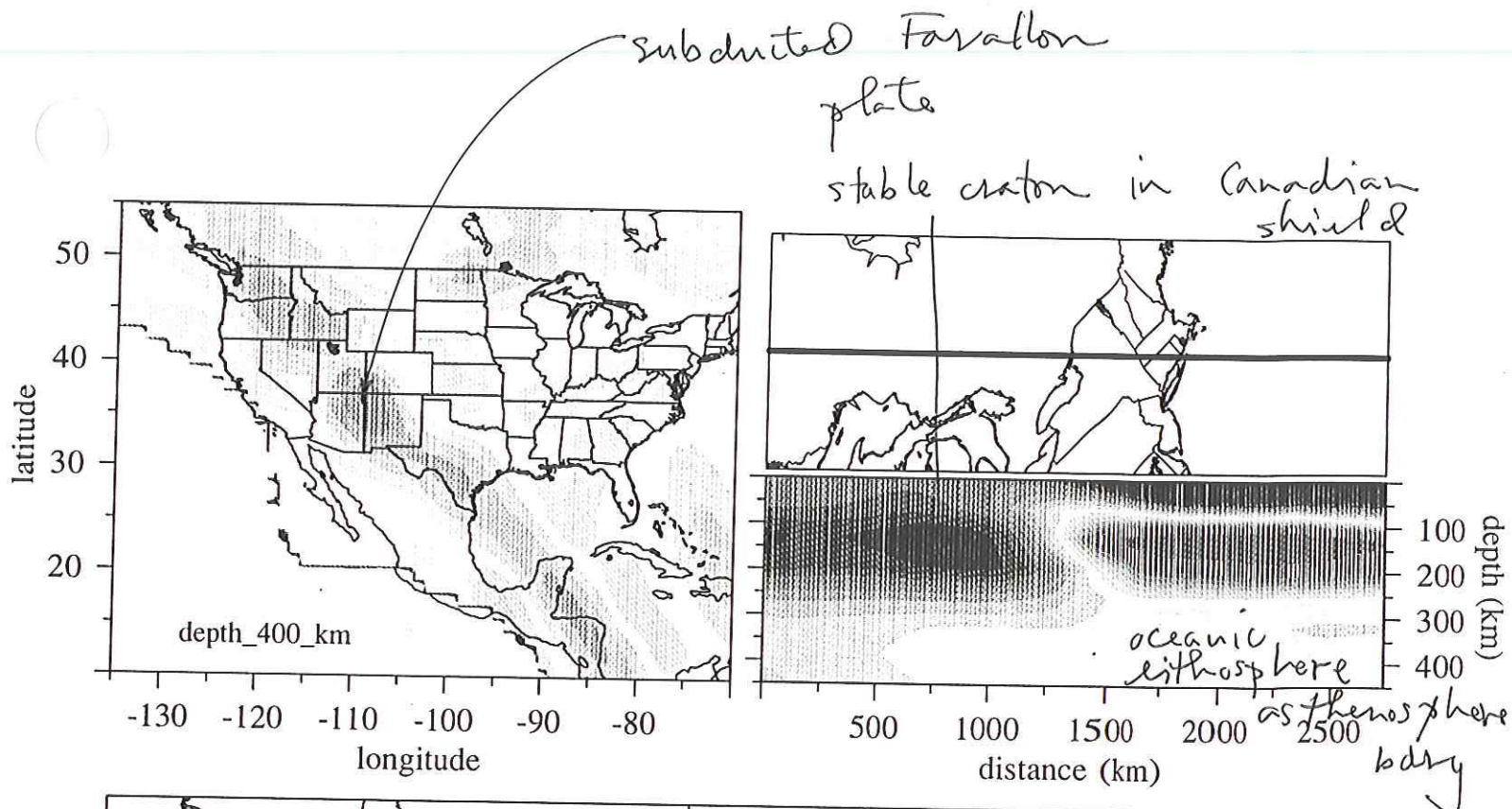


Figure 3. Lower panel: long-period S residuals plotted at the turning point of S for rays which are reflected at the lowermost 300 km of the mantle. The raw data have been lightly smoothed by applying a running-mean smoothing filter which is a spherical cap of radius 5° . Note the ring of negative residuals (fast velocity) around the Pacific. The upper panel shows a map of the data constructed using spherical splines. The contour levels are in seconds.



Don't mention Farallon plate in this lecture

Iceland root instead!

extremely precise: 0.50 :

$$T = 1227.500 \pm \text{~~0.006~~} 0.006 \text{ seconds}$$

There is very little damping associated with this almost purely compressional oscillation. Visible for weeks after a large quake.

The frequencies of the Earth's modes depend upon the density $\rho(r)$.

of course, they depend on $\alpha(r)$ and $\beta(r)$ too.

Earth-model refinements are obtained by fitting the measured frequencies and body-wave travel times simultaneously.

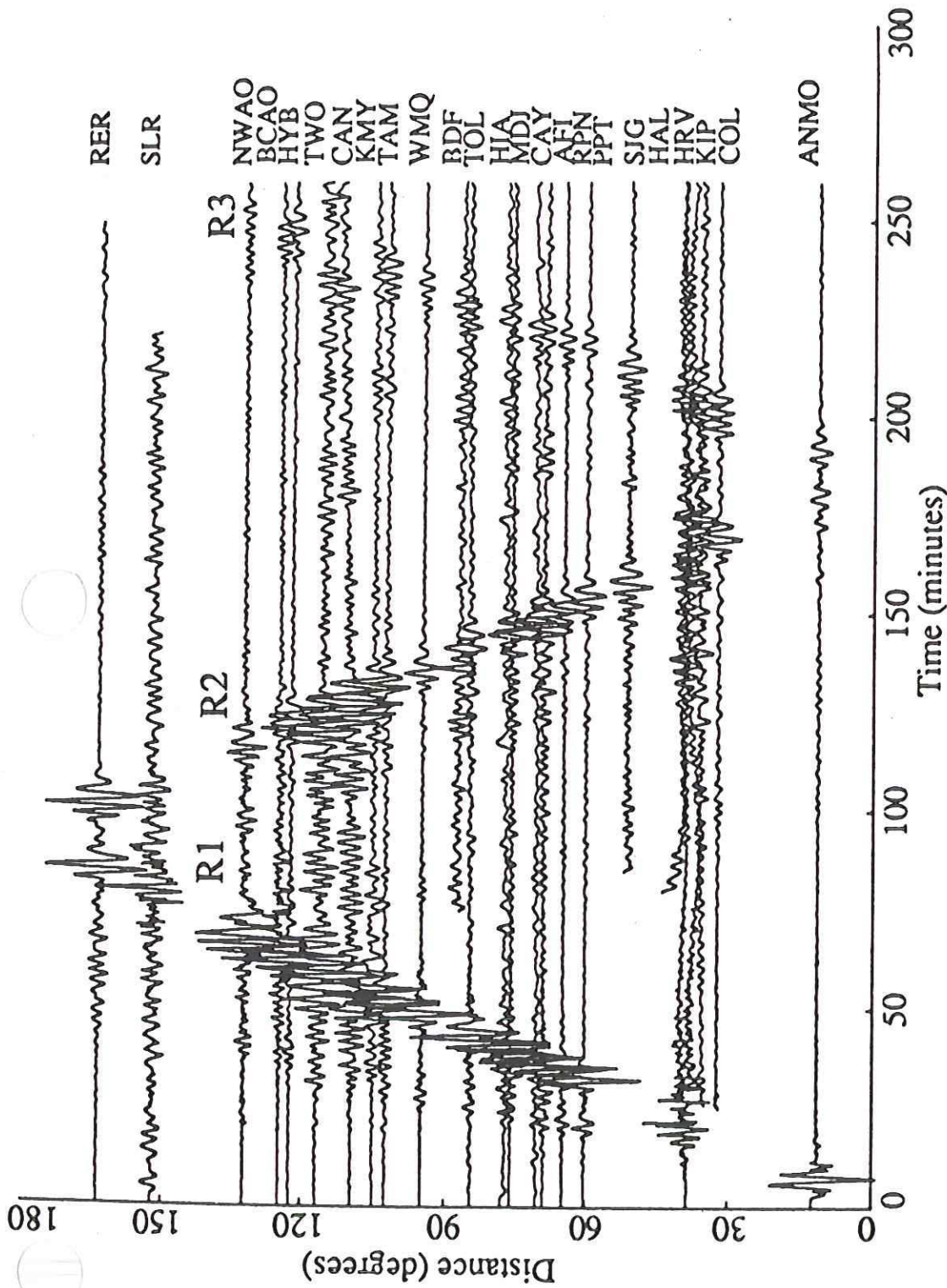


FIGURE 1.7 Long-period Rayleigh waves produced by the 1989 Loma Prieta earthquake as recorded at globally distributed digital seismometers of three global networks (GEOSCOPE, International Deployment of Accelerometers, Global Seismic Network). The vertical-component traces are filtered to include only periods longer than 125 s. The vertical axis is the angular distance along the surface from the California source, and time is from the earthquake origin time. R_1 and R_2 are Rayleigh waves traveling along the minor and major arcs of the great circle from source to station, respectively; R_3 is the next passage of the R_1 wave after circling the entire globe. (From Velasco *et al.*, 1993.)

The principal limitation is not instrument sensitivity but ground noise

microseismic noise : main source H₂O pressure fluctuations on seafloor ; also wind blowing trees , etc.

Ground noise vs frequency at 3 sites.

~~RPN on Easter Island is noisiest~~

Dominant period 6 seconds.
Much lower at longer periods but only very large 'quakes' excite long-period waves.

Noise in 1-10 s period range :

RPN : $10^{-5} \text{ m} = 10 \text{ } \mu\text{m}$ noisy site

PFO : $10^{-7} \text{ m} = \frac{1}{10} \text{ } \mu\text{m}$ quiet site

Typical signal sizes are as follow

M	wave type	displacement (μm)
7	20 s surface wave at 3000 km	100 μm
7	1 s P wave at 3000 km	40 μm
3.5	1 s S wave at 100 km	10 μm

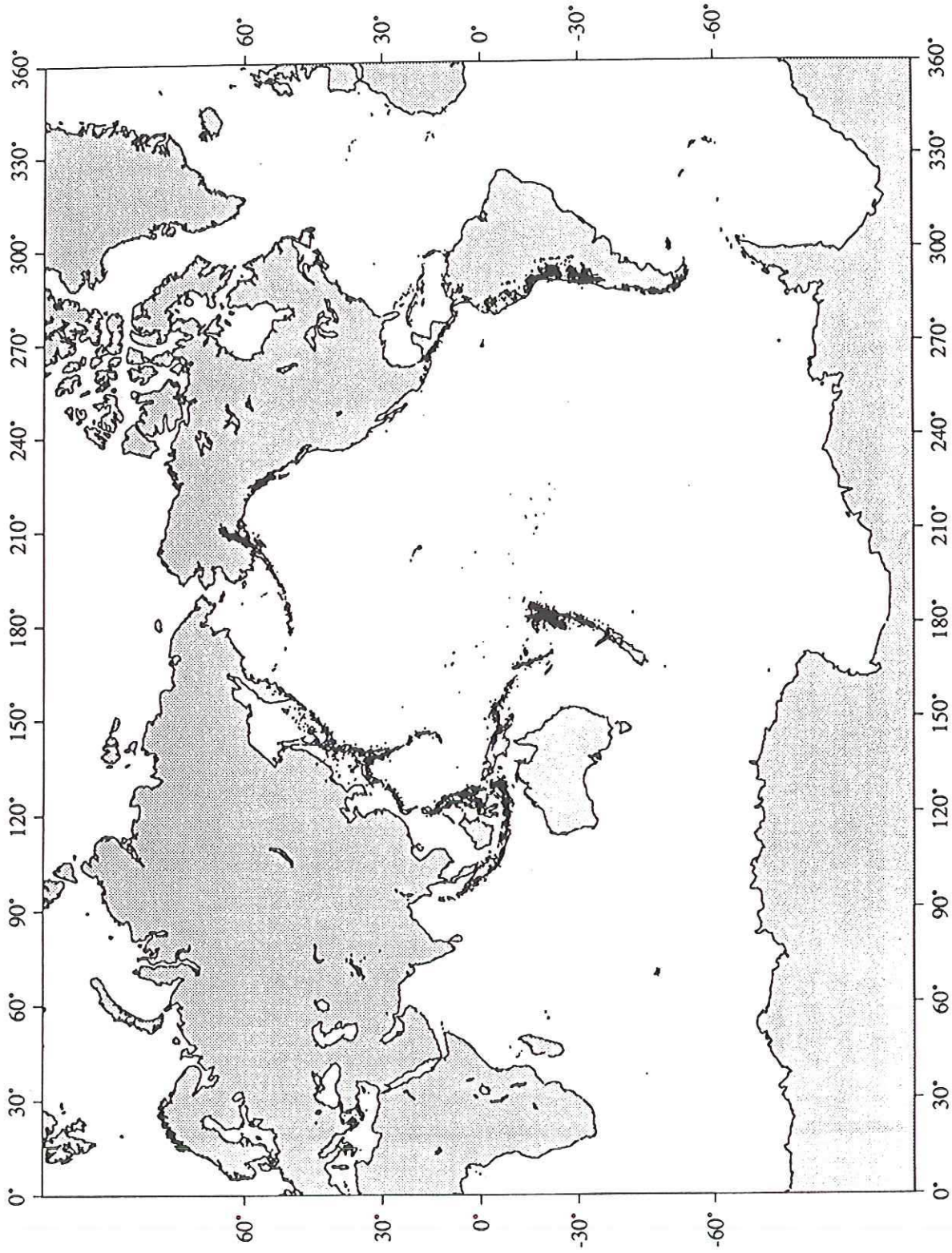


FIGURE 1.11 Maps of the distribution of earthquakes determined by the global networks for the years 1970 to 1990. At the top, the source location for events less than 100 km deep are shown; at the bottom, events with depths from 100 to 700 km are shown.

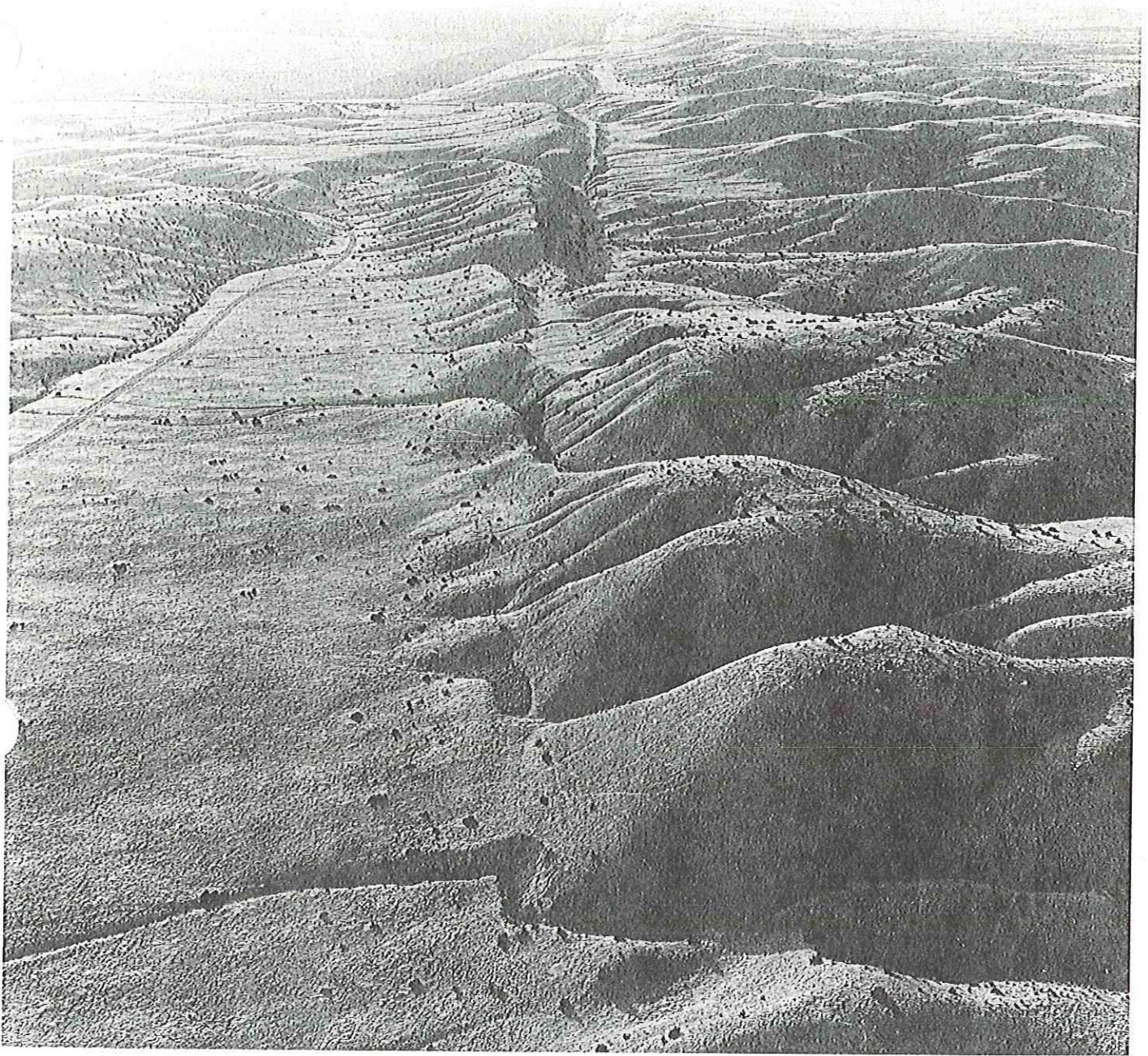
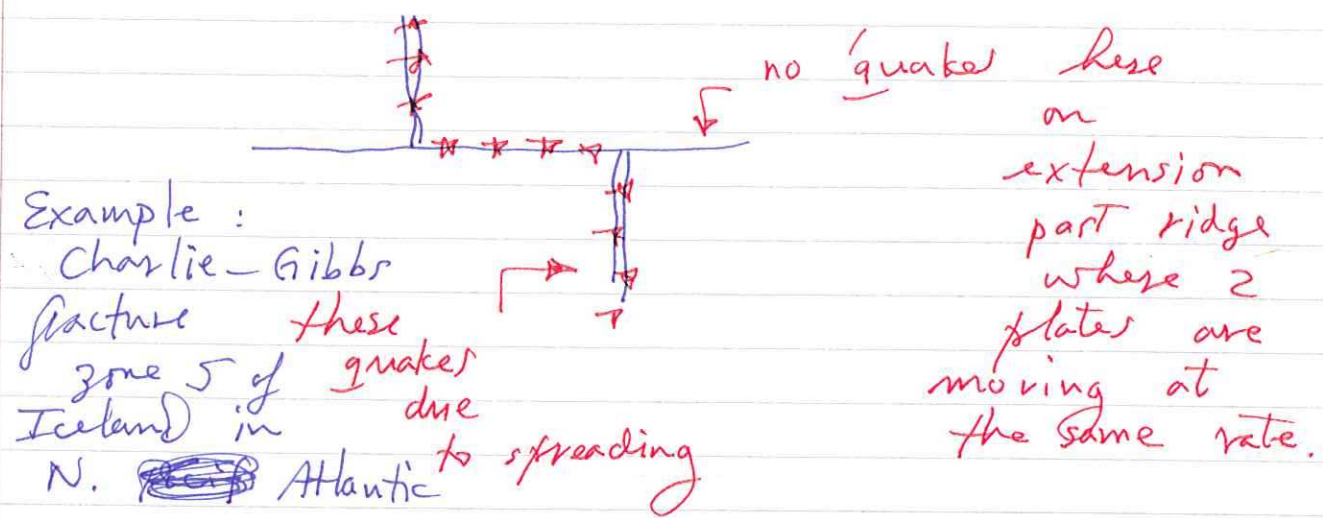


Figure 8-23. The surficial traces of strike-slip faults are commonly less irregular than those of normal and reverse faults. The extremely linear trace of the right-lateral San Andreas fault, in the Carrizo Plain of California, is a good example. View is toward the northwest, and closest channel is offset 16 m. Photo by C. R. Allen (1967).

right lateral

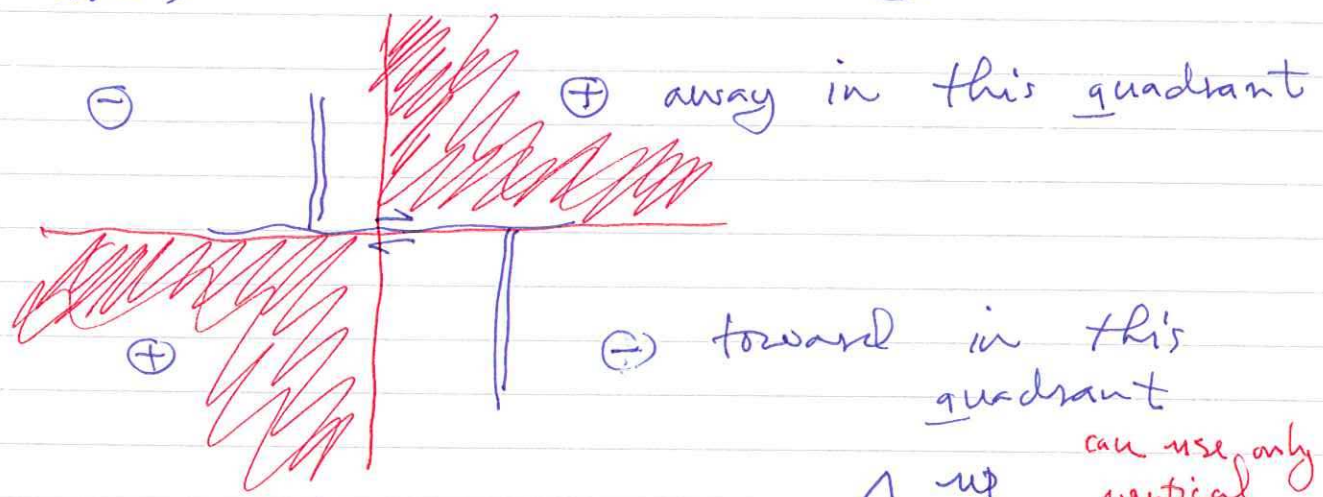
Seismology provides a test of this hypothesis

Prediction (1):

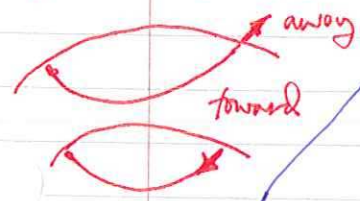


Example: Charlie-Gibbs fracture zone of quakes due to spreading in N. Atlantic

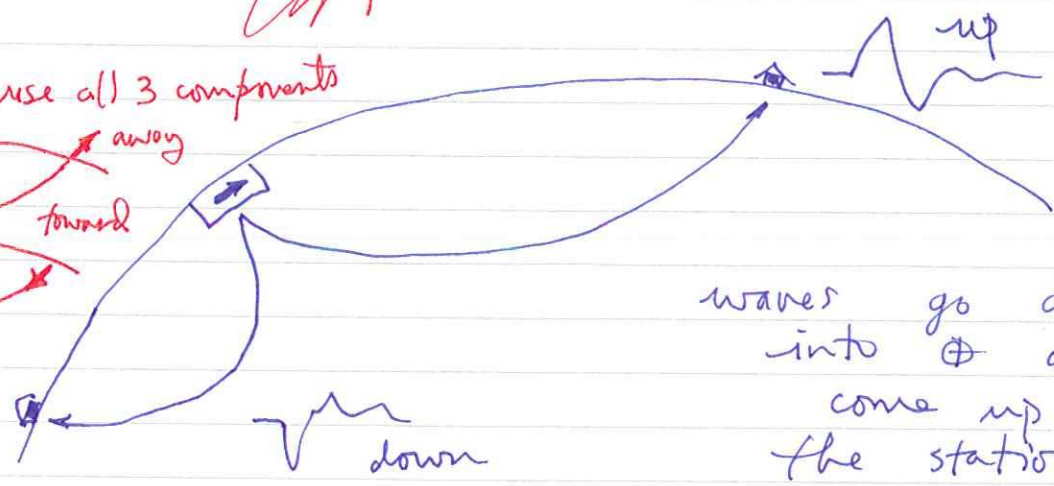
Prediction (2): "first motion" of P waves



in lab use all 3 components



can use only vertical component of ground displacement



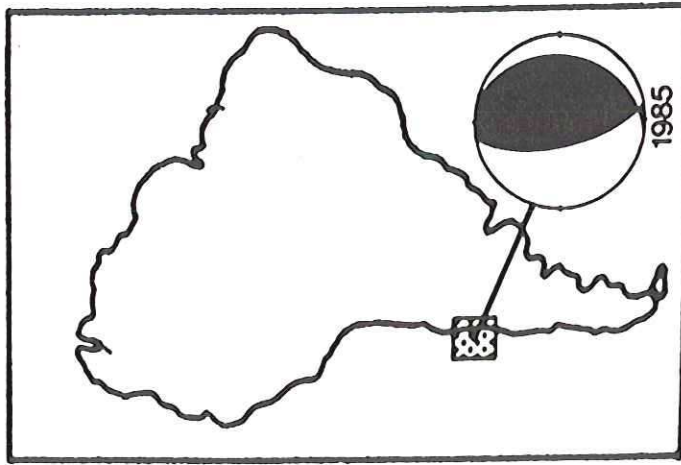
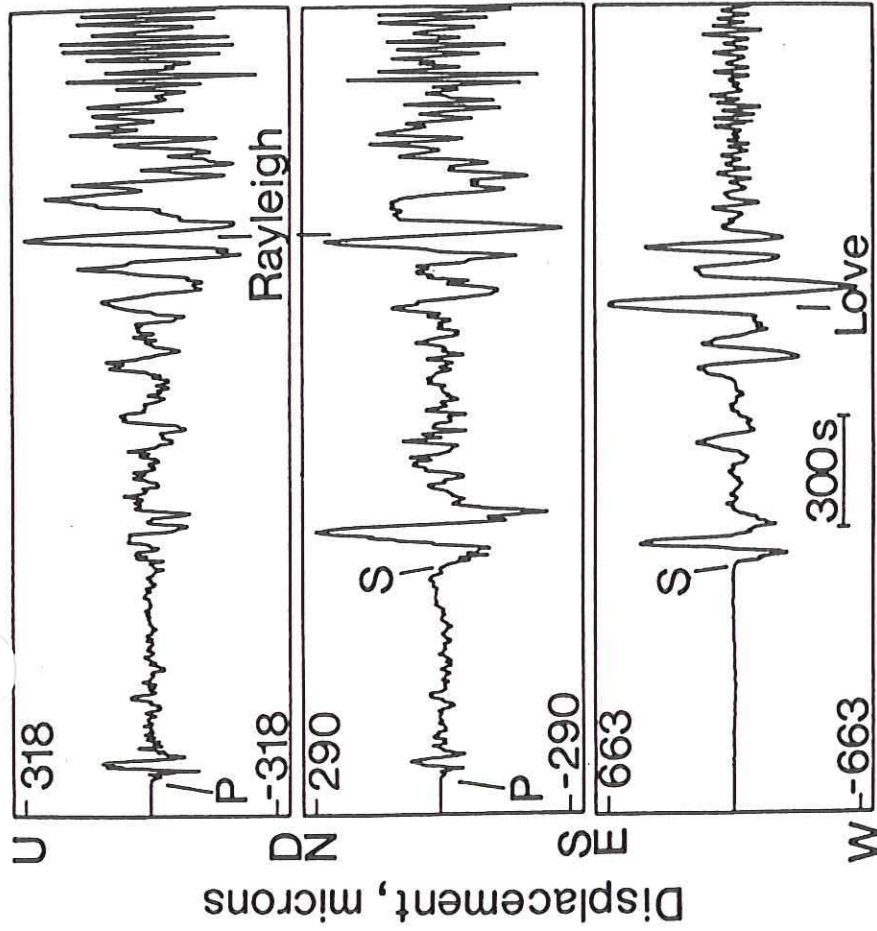


FIGURE 1.1 Recordings of the ground displacement history at station HRV (Harvard, Massachusetts) produced by seismic waves from the March 3, 1985, Chilean earthquake, which had the location shown in the inset. The three seismic traces correspond to vertical (U-D), north-south (N-S), and east-west (E-W) displacements. The direction to the source is almost due south, so all horizontal displacements transverse to the raypath appear on the east-west component. The first arrival is a *P* wave that produces ground motion along the direction of wave propagation. The *S* motion is large on the horizontal components. The Love wave occurs only on the transverse motions of the E-W components, and the Rayleigh wave occurs only on the vertical and north-south components. These motions are consistent with the predictions of Figure 1.2. (Modified from Steim, 1986.)

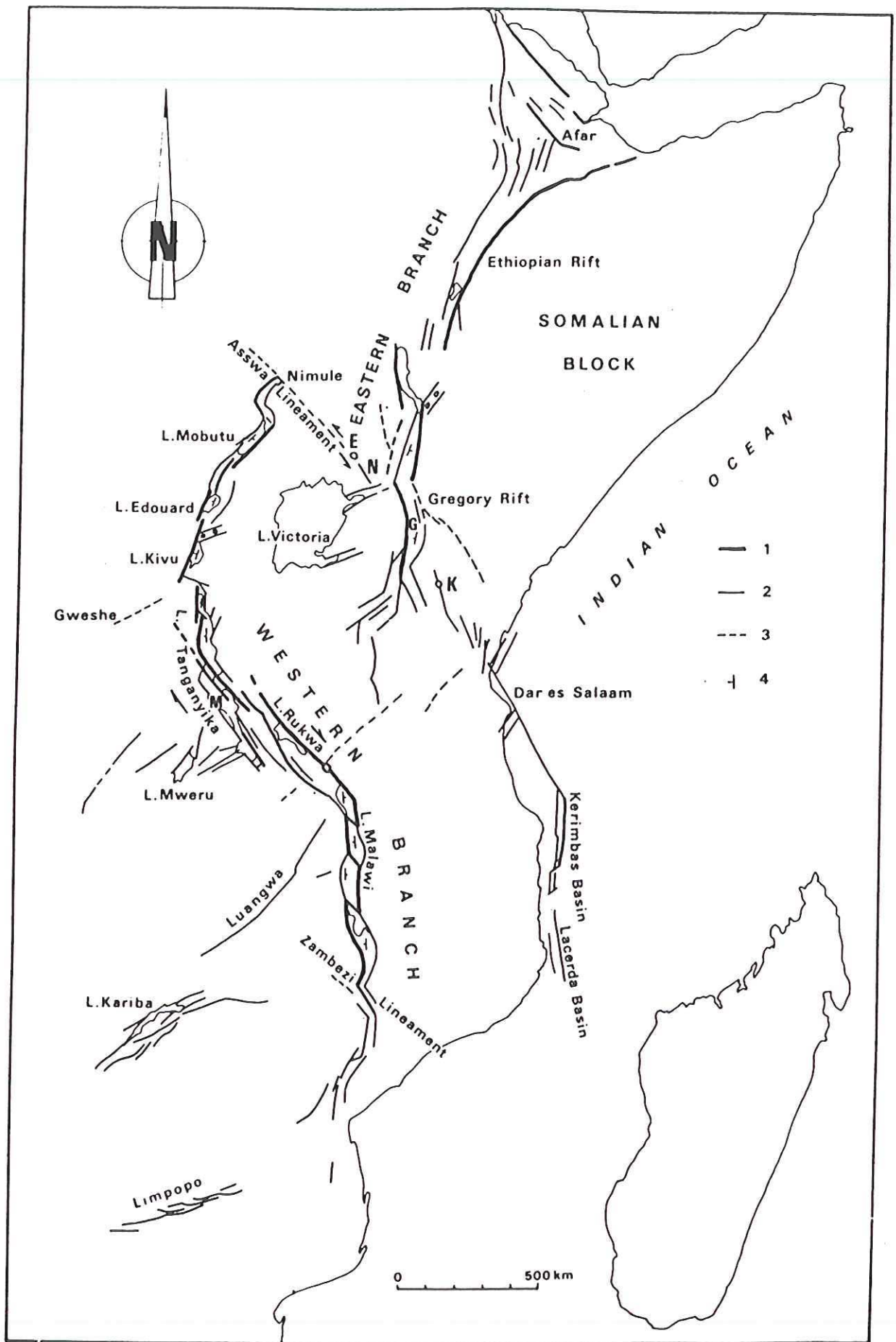


FIGURE 11.10 Major tectonic features of the East African Rift. The rift has two branches, which merge in Ethiopia; the East African Rift joins the Red Sea Rift at Afar. The Red Sea was formerly continental, but now it is completely floored by oceanic crust. (Reprinted from Chorowicz, J., 1989, pp. 203–214, with kind permission from Elsevier Science Ltd., The Boulevard, Langford Lane, Kidlington OX5 1GB, UK.)

Measure ground deformation in units of wavelength of radar wave

Example - earthquake in Greece

Method developed by French group in Toulouse

Imaging slip distribution on the fault

By careful analysis of close-in stations can infer details of faulting

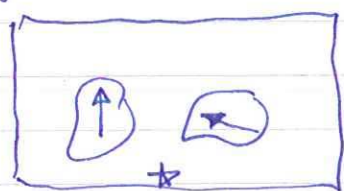
slip history $s(x, y, t)$
↑
time

Three examples:

(1) Beroza - Loma Prieta - World Series interrupted in Candlestick Park $M = 7.0$

occurred on a dipping segment of San Andreas fault

1989

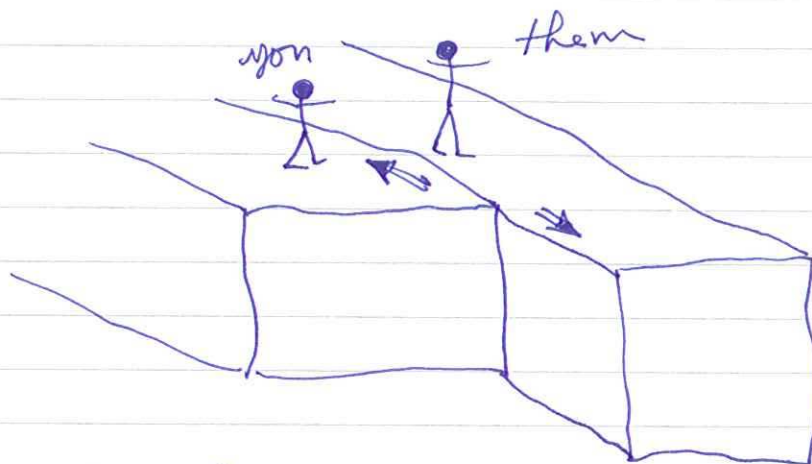


nucleation at 14 km depth

maximum ~~slip~~ dip slip ~~4.4 m~~ 4.4 m

maximum strike slip 5.5 m

So, if you were standing on the fault talking to someone and it started slipping



You would have to walk at 1 m/sec to keep up.

Faults slip at about the speed you can walk

(3) 1995 Kobe quake - Wald

Nucleates at 17 km - bilateral propagation

$$v = 2.8 \text{ km/sec}$$

rupture duration 12 sec

max slip 3.5 m - average slip 1-2 m

local slip duration 1-2 sec

→ slip rate
1 m/sec

Week 6 - Lecture #2 - last lecture before exam - plate tectonics

1960's ~~the~~ time of installation of WWSSN - global seismic network for monitoring underground nuclear explosions

Kennedy - Kruscher LTBT 1963 drove testing underground

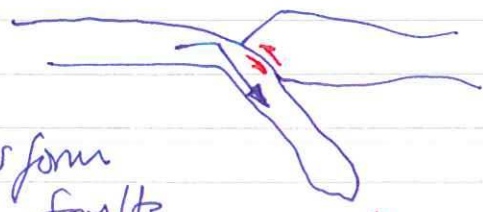
First reliable map of global seismicity - outlined the major plates

Plate tectonics synthesized these various threads - developed by D. McKenzie (Cambridge) and Jason Morgan (Princeton)

Earth's surface divided into about a dozen quasi-rigid plates.

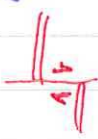
Three types of plate boundaries

- (1) mid-ocean ridges where seafloor is created
- (2) ~~transform faults~~ subduction zones where it is destroyed



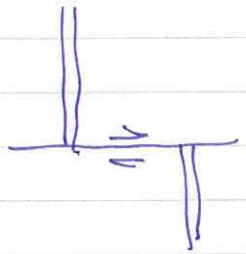
(3) transform faults

offsetting MOR but frequently not always



Current plate Motions — do this first, then Pacific Margin evolution and motion of India
Rates of plate motion can be measured along ridges.

Directions can be measured by noting the strikes of transform faults



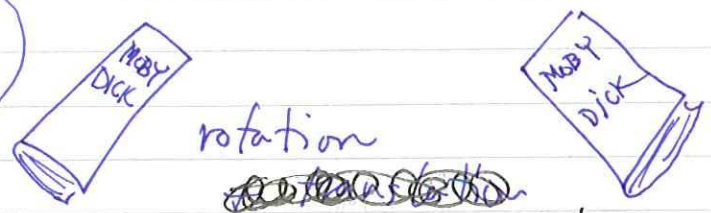
Also by ~~mechanisms~~ using earthquake focal mechanisms at subduction zones.
Over 10,000 of these at present time

Motions on a sphere: governed by Euler's theorem

On a flat plane

Be sure to take a copy of J&R as a proof.

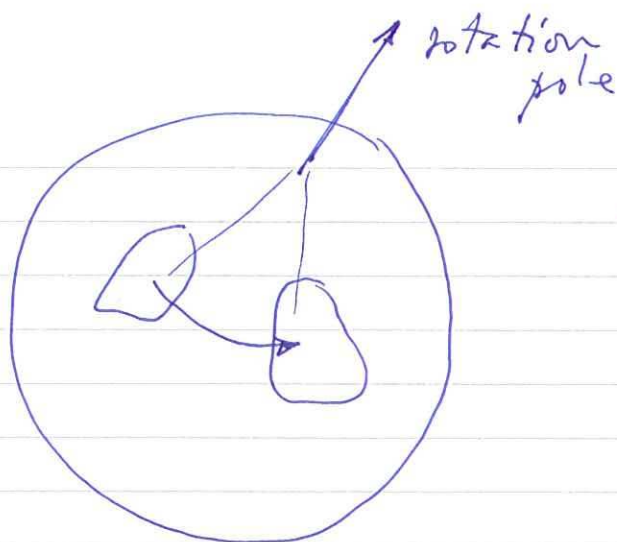
every rigid motion is a rotation — pole + rate
 θ, ϕ
i.e.
3
variables



rotation
~~translation~~
translation \equiv rotation about a pole at ∞

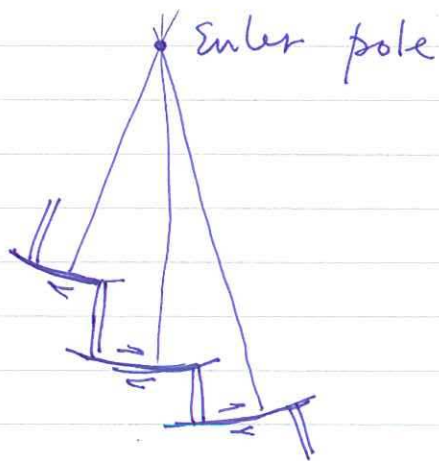
(Also true on a sphere: only a rotation is required.)

True in 2D, not 3D.



Euler's theorem — every rigid motion of a plate on a sphere can be described by a rotation about a rotation pole

The transform faults between two plates define the rotation pole ~~describing~~ describing their relative motion



By putting this information together can compile a complete picture of present-day ~~plate motions~~ relative plate motions

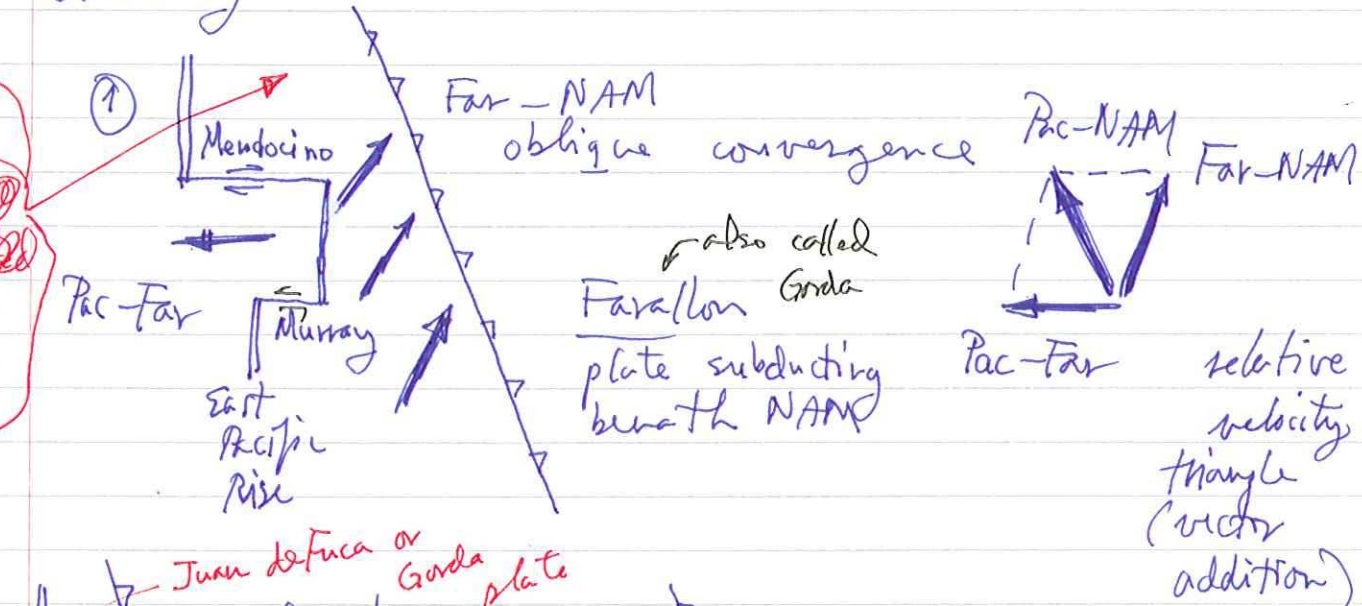
Discuss present-day (NUVEL-1) first then reconstruction of past.

Fig 12.38 in book

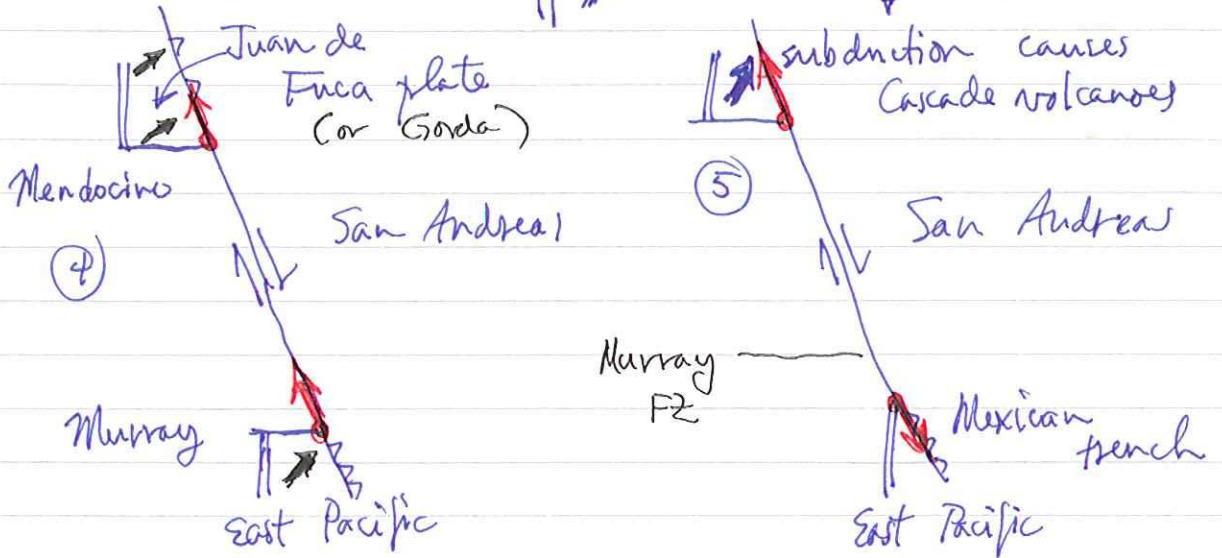
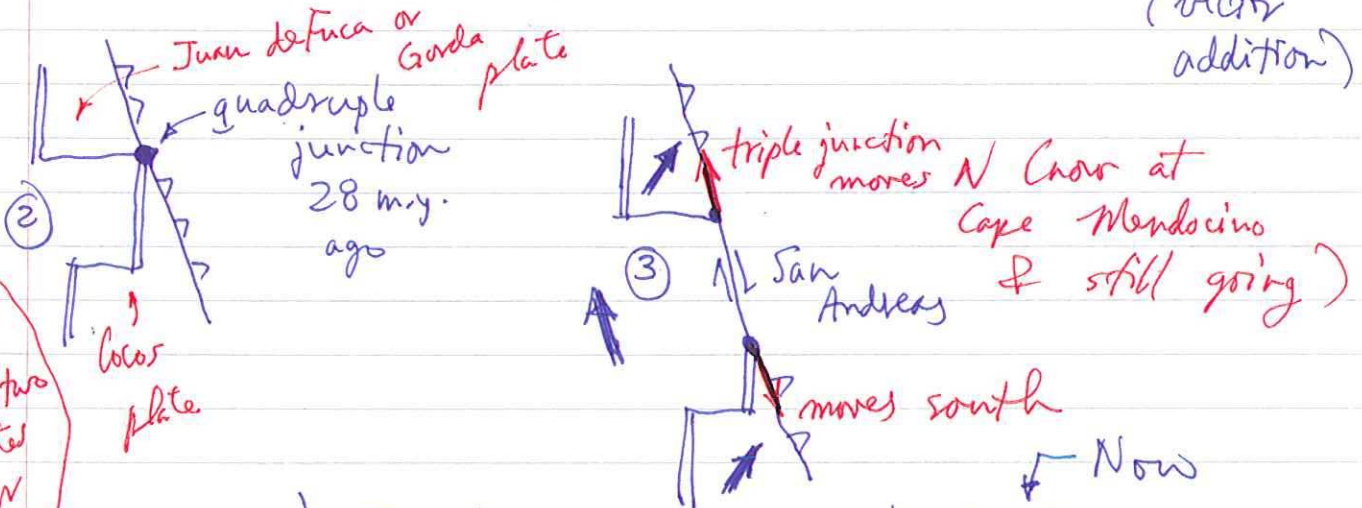
Scenario for evolution of San Andreas Fault:

In the Oligocene (30 m.y. ago) the Pacific Coast boundary of Calif. was a subduction boundary

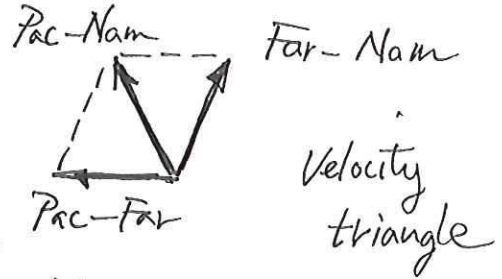
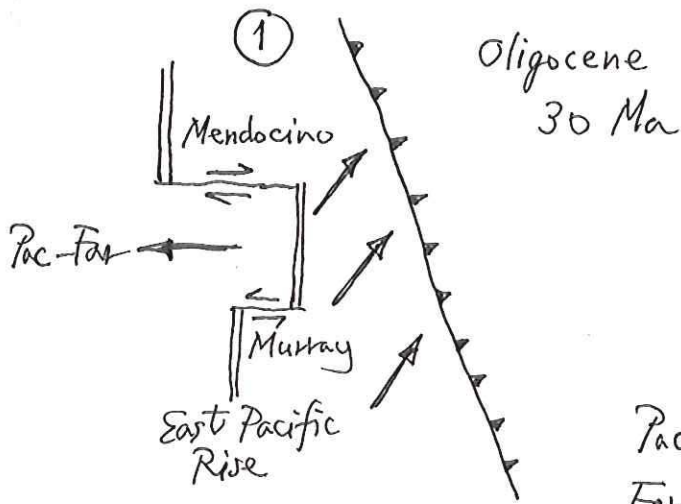
Farallon Plate



Farallon "splits" into two plates 28 Myr ago



Evolution of the California Margin



Pac: Pacific plate
Far: Farallon plate
Nam: North American plate

